Ginsenoside 20(S)-Rg3 inhibits the Warburg effect through STAT3 pathways in ovarian cancer cells

JIE LI[1*], TING LIU[1*], LE ZHAO[1], WEI CHEN[2], HUILIAN HOU[3], ZHONGXUE YE[1] and XU LI[1]

Centers for [1]Translational Medicine and [2]Laboratory Medicine, [3]Department of Pathology, The First Affiliated Hospital, School of Medicine, Xi'an Jiaotong University, Xi'an, Shaanxi 710061, P.R. China

Received September 24, 2014; Accepted October 30, 2014

DOI: 10.3892/ijo.2014.2767

Abstract. Cancer cells prefer to metabolize glucose through aerobic glycolysis, known as the Warburg effect. It plays a crucial role in proliferation and progression of cancer cells. However, the complete mechanism remains elusive. In recent studies, the signal transducer and activator of transcription 3 (STAT3) signaling has been discovered to have roles in cancer-associated changes in metabolism. In this study, we find that the ginsenoside 20(S)-Rg3, a pharmacologically active component of the traditional Chinese herb Panax ginseng, inhibits glycolysis in ovarian cancer cells by regulating hexokinase 2 (HK2) and pyruvate kinase M2 (PKM2). We also show that 20(S)-Rg3 regulates HK2 through down-regulation of p-STAT3 (Tyr705). Furthermore, overexpression of STAT3 in ovarian cancer cells weakened the suppression of Warburg effect induced by 20(S)-Rg3. Importantly, 20(S)-Rg3 treatment represses HK2 expression in nude mouse xenograft models of ovarian cancer. Taken together, our results show that 20(S)-Rg3 inhibits the Warburg effect by targeting STAT3/HK2 pathway in ovarian cancer cells, highlighting the potentiality of 20(S)-Rg3 to be used as a therapeutic agent for ovarian cancer.

Introduction

Ovarian cancer, the most lethal gynecologic malignancy, exists predominantly in the form of epithelial ovarian cancer (EOC) (1,2). In the United States, EOC is the leading cause of death among gynecologic malignancies with ~22,280 cases and 15,500 deaths every year (3). Despite the use of aggressive treatment, most EOC patients develop recurrent cancer, and cancer metastasis is one of the leading causes of death.

Ginsenosides are the pharmacologically active components of Panax ginseng (4) that has long been utilized as a traditional Chinese medicine for officinal or recuperative purposes (5,6). To date, >100 ginsenoside compounds have been identified (7), among which the stereoisomer Rg3 is one of the bioactive extracts with antitumor effect (8,9). It is reported that Rg3 could play multiple roles similarly to other ginsenosides, including anti-inflammation properties (10,11), inhibiting scar hyperplasia of skin (12) and angiogenesis (13). Furthermore, accumulating evidence supports that Rg3 could become a new medicine for cancer preventionin, because it can inhibit cancer growth, metastasis and development (8,9), but the mechanisms are still unclear. Ginsenoside Rg3 has two optically active chiral molecules 20(R)-Rg3 and 20(S)-Rg3, which differ in the orientation of the hydroxyl (OH) group on carbon-20 (5). Although both were reported to inhibit tumor metastasis (8), stereospecifity of Rg3 appears to be linked to their bioactivities (6). In our preliminary studies (unpublished), 20(S)-Rg3 robustly blocked EMT process in ovarian cancer. In this study, we discovered for the first time that 20(S)-Rg3 effectively inhibits the Warburg effect of human ovarian cancer cells, promising a novel natural agent for anti-ovarian cancer therapy.

The Warburg effect, which was first described by Warburg in the 1930s, is a metabolic reprogramme used by cancer cells to support their high energy requirements and high rates of macromolecular synthesis (14,15). In cancer cells, the main hallmark of the Warburg effect is aerobic glycolysis, in which glucose consumption and lactate production are both increased even in the presence of oxygen (16). The Warburg effect not only allows cancer cells to meet their high energy demands and supply the anabolic precursors for nucleotide and lipid synthesis, but it also minimizes reactive oxygen species production in mitochondria, thereby providing a growth advantage for tumors. Since Warburg effect plays a crucial role in proliferation and progression of cancer cells, it provides a novel target for anticancer therapy.

The mechanism of Warburg effect is also complicated, because Warburg effect could be impacted by many factors. There is evidence that the signal transducer and activator of transcription 3 (STAT3) is involved in Warburg effect. STAT3 has emerged as a potential anti-cancer target as it is crucial

Correspondence to: Professor Xu Li, Center for Translational Medicine, The First Affiliated Hospital, School of Medicine, Xi'an Jiaotong University, 28 Xianning West Rd, Xi'an, Shaanxi 710061, P.R. China
E-mail: lixu56@mail.xjtu.edu.cn

*Contributed equally

Key words: 20(S)-Rg3, STAT3, Warburg effect, ovarian cancer

in the regulation of genes involved in cell proliferation and survival, and is constitutively activated in common human cancers (17,18). STAT3 can be phosphorylated by tyrosine kinase which is activated by cytokines, growth factors, or hormones (19). In ovarian cancer, STAT3 siRNA downregulates cyclin D1, survivin, and vascular endothelial growth factor expression in HOC cells; inhibits STAT3 and its related genes; inhibits HOC cell growth; and induces apoptosis *in vitro* (20). Recent studies have found that STAT3 was also involved in regulating glycolysis. In breast cancer cells, the activation of STAT3 can combine to hexokinase 2 (HK2) promoter, and then promote HK2 transcription activation, regulate aerobic glycolysis of breast cancer cells (21). Sustained activation of STAT3 can promote glycolysis and inhibit mitochondrial function in two ways (22). As a nuclear transcription factor c-myc can participate in regulating the glycolytic pathway by regulating a variety of enzymes (23), and c-myc is also involved in STAT3 signaling network (24). Interleukin-6 (IL-6)-STAT3 signaling pathway can affect glycolysis through regulating HK2 and PFKFB3 (25). Therefore, STAT3 plays an important role in regulating the Warburg effect.

We discovered that 20(S)-Rg3 significantly inhibits the Warburg effect in ovarian cancer cells and confirmed that this process depends on the activation of STAT3. This will add to our understanding of human ovarian cancer and provide future clinical approaches to treat this disease.

Materials and methods

Reagents and antibodies. Ginsenoside standard 20(S)-Rg3 was purchased from Ambo Institute (Seoul, South Korea) and dissolved at a concentration of 50 mg/ml in DMSO as a stock solution (stored at -20˚C). It was then further diluted in cell culture medium to create working concentrations. The maximum final concentration of DMSO was <0.1% for each treatment, and was also used as a control. Other antibodies such as pyruvate kinase M2 (PKM2), HK2, phospho-STAT3 (Tyr705), and STAT3 were from Cell Signaling Technology, Inc. (Beverly, MA, USA).

Cell culture and 20(S)-Rg3 treatment. Human ovarian cancer cell lines SKOV3 (obtained from ATCC, Manassas, VA, USA) and 3AO (purchased from the Chinese Academy of Sciences Type Culture Collection, Shanghai, China) were maintained in RPMI-1640 medium (Gibco-BRL, Gaithersburg, MD, USA) supplemented with 10% (v/v) fetal bovine serum, 1% penicillin antibiotics-antimycotics at 37˚C under a humidified 5% CO_2 atmosphere. Cells were incubated with 160 μg/ml (SKOV3) and 80 μg/ml (3AO) concentrations of 20(S)-Rg3 for 24 or 48 h.

Plasmid and transient transfection. The human STAT3 expression vector pcDNA3 hId1 (POSE230074807) was purchased from GeneChem (Shanghai, China), ovarian cancer cells were seeded into 6-well plates until 80% confluent and transiently transfected with pcDNA3 hId1 or empty vector (pcDNA3) as a control using X-tremeGENE HP DNA Transfection Reagent (Roche Diagnostics, Indianapolis, IN, USA) following the manufacturer's instructions. After 48 h of transfection, the cells were harvested for further study.

Quantitative real-time PCR. Total RNA was isolated using TRIzol reagent (Invitrogen Life Technologies, Carlsbad, CA, USA) according to the manufacturer's instructions. For mRNA detection, first-strand cDNA was synthesized using a PrimeScript RT Reagent kit (Perfect Real Time; Takara Bio, Inc., Liaoning, China). Quantitative real-time PCR was performed using a SYBR Premix Ex Taq™ II kit (Takara Bio, Inc.) on a CFX96 real-time PCR system (Bio-Rad, Hercules, CA, USA). β-actin was used as an internal control to normalize the results. Gene expression was normalized to internal controls, and fold changes were calculated using relative quantification ($2^{-\Delta\Delta Ct}$).

Western blot analysis. Cell lysates were collected using Mammalian Protein Extraction Reagent (Pierce Biotechnology, Inc., Rockford, IL, USA) containing protease inhibitors (Roche Diagnostics). The protein concentrations in each sample were determined using the BCA-200 Protein Assay kit (Pierce Biotechnology, Inc.). The proteins were resolved on 12 or 10% (for other protein detection) SDS-polyacrylamide gels and transferred onto nitrocellulose membranes. The membranes were then blocked using blocking buffer (5% non-fat milk in TBST) and incubated overnight at 4˚C with rabbit anti-human PKM2 (no. D78A4), HK2 (no. C64G5), phospho-STAT3 (Tyr705) (no. 9139), and STAT3 (no. 9145), and mouse anti-human β-actin (no. 3700S) (all from Cell Signaling Technology, Inc.) at dilutions of 1:2,000, 1:500, 1:500, 1:500, and 1:1,000, respectively. After washing with TBST, the blots were visualized using peroxidase (HRP)-conjugated anti-rabbit or anti-mouse IgG and ECL reagents (Pierce Biotechnology, Inc.).

Immunohistochemical staining. Paraffin-embedded mouse ovarian cancer tissue sections on Poly-L-Lysine-coated slides were deparaffinized and rinsed with 10 mM Tris-HCl (pH 7.4) and 150 mM sodium chloride. Paroxidase was quenched with methanol and 3% hydrogen peroxide. Slides were then placed in 10 mM citrate buffer (pH 6.0) at 100˚C for 20 min in a pressurized heating chamber. After incubation with 1:50 dilution of rabbit monoclonal antibody to HK2 (no. C64G5), or with 1:800 dilution of rabbit monoclonal antibody to PKM2 (no. D78A4) (both from Cell Signaling Technology, Inc.) for 1 h at room temperature, slides were thoroughly washed three times with phosphate-buffered saline. Bound antibodies were detected using the EnVision Detection Systems Peroxidase/DAB, Rabbit/Mouse kit (Dako, Glostrup, Denmark). The slides were then counterstained with hematoxylin.

Glucose consumption and lactate production assay. To determine the levels of glucose and lactate, the supernatants of cell culture media were collected and detected using a glucose and lactate assay kit (BioVision, Inc., Milpitas, CA, USA) according to the manufacturer's instructions. The values at different time periods were analyzed by the optical density values. Glucose consumption and lactate production were calculated based on the standard curve, and normalized to the cell number.

Statistical analysis. All experiments were performed at least in triplicate, and each experiment was independently performed

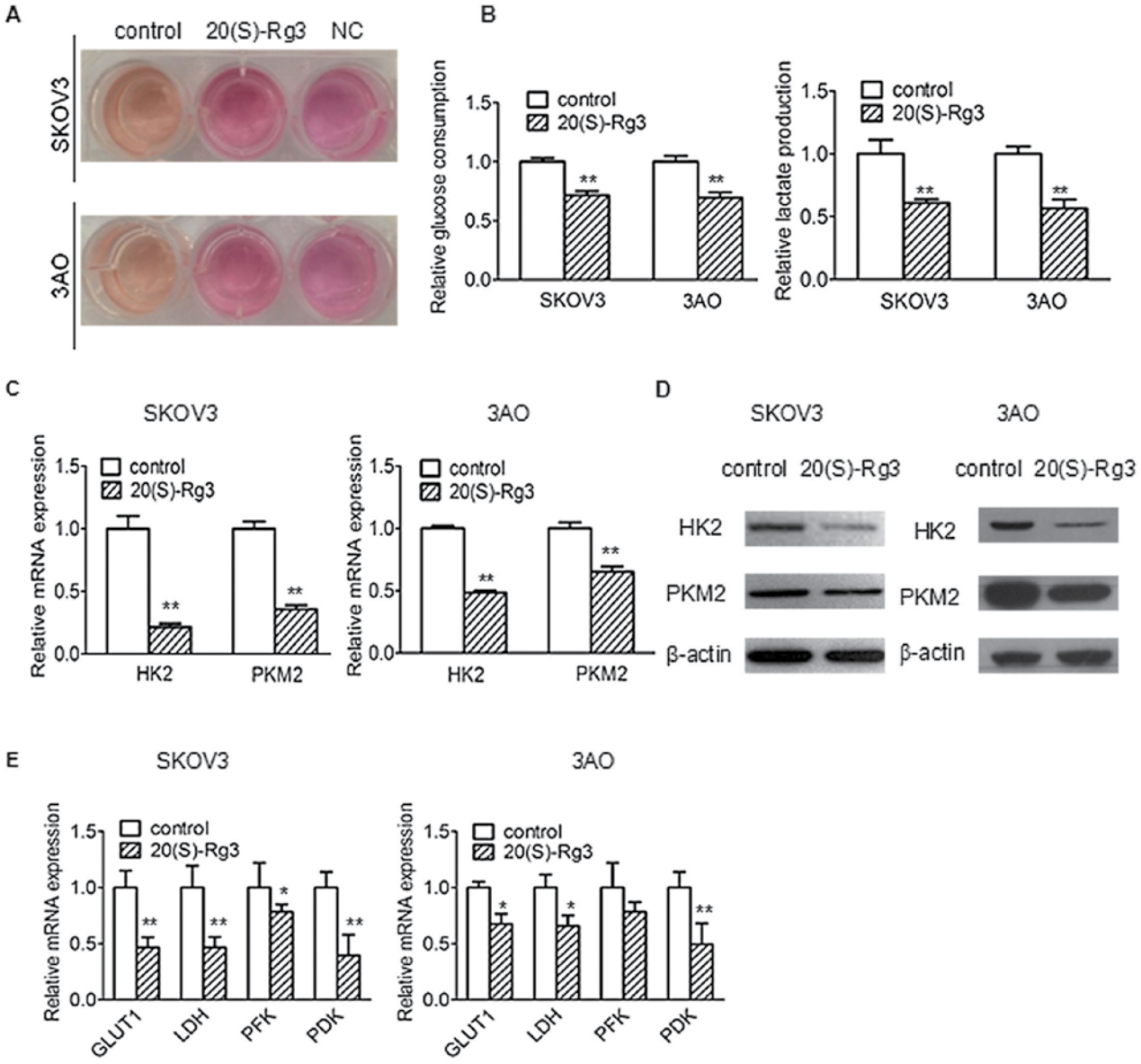

Figure 1. 20(S)-Rg3 induces a metabolic shift in SKOV3 and 3AO ovarian cancer cells. (A) SKOV3 and 3AO cells expressing either control or 20(S)-Rg3 were cultured for 24 h. Acidification of the culture medium was evaluated by visually inspecting the color of the medium. NC, the culture medium of 20(S)-Rg3 without cells. (B) SKOV3 and 3AO cells expressing either control or 20(S)-Rg3 were cultured for 24 h. Levels of lactate in the culture medium and glucose consumption were then measured and normalized to cell number. (C) Real-time RT-PCR analysis shows that the expression of hexokinase 2 (HK2) and pyruvate kinase M2 (PKM2) is downregulated in SKOV3 and 3AO cells treated by 20(S)-Rg3 for 24 h. (D) Western blot assays show that the expression of HK2 and PKM2 is downregulated in SKOV3 and 3AO cells treated by 20(S)-Rg3 for 48 h. (E) Real-time RT-PCR analysis shows that the expression of other metabolic enzyme genes are downregulated in SKOV3 and 3AO cells treated by 20(S)-Rg3 for 24 h. All of the treatments shwn in this figure were carried out in triplicate, and the results are reported as the means ± standard deviation (SD). *P<0.05, **P<0.01, t-test. GLUT1, glucose transporter; LDH, lactate dehydrogenase; PFK, phosphofructokinase; PDK, pyruvate dehydrogenase kinase.

at least three times. Data are presented as the means ± standard deviation (SD) and were analyzed using SPSS 19.0 and GraphPad Prism 5 software. Statistical significance was assessed using the two-tailed unpaired Student's t-test. Differences were considered statistically significant when the P-value was <0.05.

Results

20(S)-Rg3, but not 20(R)-Rg3 induces a metabolic shift in SKOV3 and 3AO ovarian cancer cells. In cancer cells, glucose is preferentially metabolized by aerobic glycolysis, which differs from mitochondrial oxidative phosphorylation in normal, non-tumourigenic cells. This phenomenon, termed the Warburg effect, is characterized by increased glycolysis and lactate production regardless of oxygen availability. In our study, we first examined whether 20(S)-Rg3 or 20(R)-Rg3 was capable of inducing a metabolic shift in two human ovarian cancer cell lines SKOV3 and 3AO. We found that 20(S)-Rg3 inhibited glucose uptake and lactate secretion >30% (Fig. 1B) and reduced the acidity of cell culture media (Fig. 1A), but 20(R)-Rg3 had no effect on glucose uptake, lactate secretion and metabolic enzyme genes (Fig. 2). *HK2* and *PKM2* are key cell glycolysis genes. The RT-qPCR analysis and western blot analysis showed that 20(S)-Rg3 inhibited the expression of HK2 and PKM2 (Fig. 1C and D). 20(S)-Rg3 can also inhibit

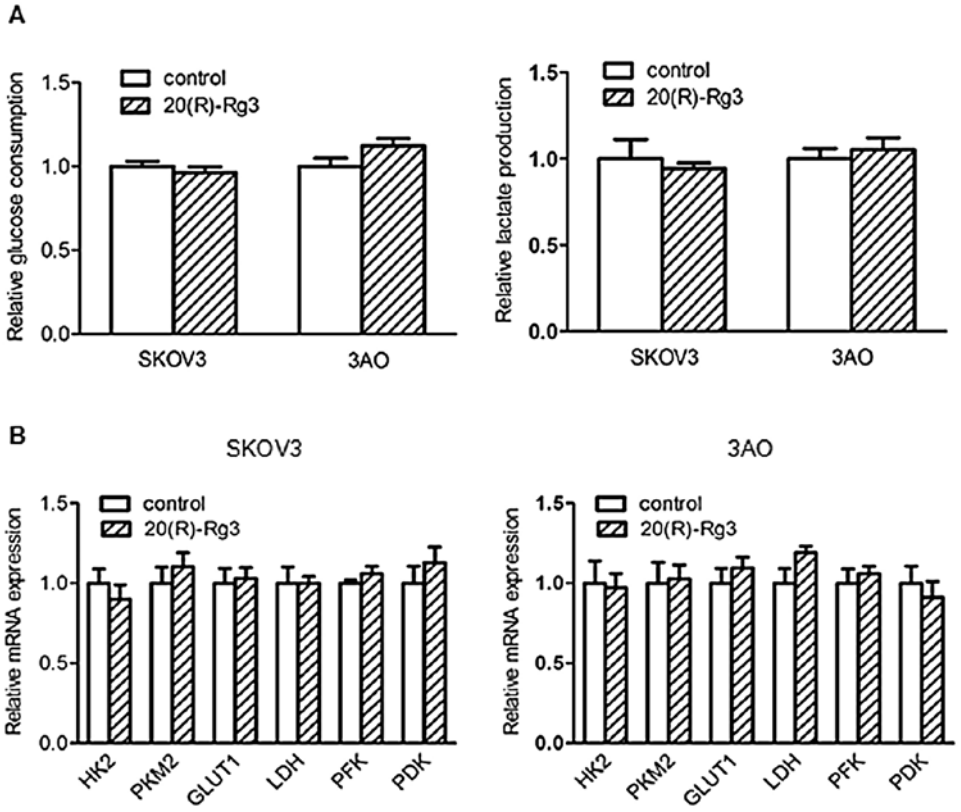

Figure 2. The effect on glucose uptake, lactate secretion and metabolic enzyme genes of 20(R)-Rg3. (A) SKOV3 and 3AO cells expressing either control or 20(R)-Rg3 were cultured for 24 h. Levels of lactate in the culture medium and glucose consumption were then measured and normalized to cell number. (B) Real-time RT-PCR analysis shows that the expression of metabolic enzyme genes is regulated in SKOV3 and 3AO cells treated by 20(R)-Rg3 for 24 h. All of the treatments reported in this figure were carried out in triplicate, and the results are the means ± standard deviation (SD). *P<0.05, **P<0.01, t-test.

other metabolic enzyme genes including *GLUT1*, *LDH*, *PDK* and *PFK* in Warburg effect (Fig. 1E).

Downregulation of p-STAT3 contributes to the inhibition of Warburg effect by 20(S)-Rg3 in SKOV3 and 3AO cells. Previously (Fig. 3B) we found that STAT3 was also involved in regulating glycolysis. Thus, we further confirmed that STAT3 played an important role in Warburg effect of SKOV3 and 3AO cells. We found that 20(S)-Rg3 downregulated p-STAT3 (Y705) without STAT3 in SKOV3 and 3AO cells (Fig. 3A). To demonstrate the role of STAT3 in 20(S)-Rg3-induced metabolic shift in ovarian cancer cells, STAT3 was ectopically transfected into SKOV3 and 3AO cells. Overexpression of STAT3 significantly promoted glucose uptake and lactate secretion and reduced the effects of 20(S)-Rg3 on glucose uptake and lactate secretion in SKOV3 and 3AO cells (Fig. 3B). In a previous study (Fig. 1C and E), the expression of HK2 had the greatest reduction after 20(S)-Rg3 treatment, so we chose HK2 for further study. The RT-qPCR and western blot analysis showed that overexpression of STAT3 significantly promoted HK2 and reduced the effects of 20(S)-Rg3 on expression of HK2 (Fig. 4). These results indicated that STAT3 plays an important role in the process of aerobic glycolysis regulated by 20(S)-Rg3 in SKOV3 and 3AO cells.

Expression of HK2 and PKM2 in ovarian cancer tissue subcutaneous tumors of nude mice. In preliminary studies (unpublished), we found that 20(S)-Rg3 inhibited growth of xenografts of ovarian cancer in nude mice. Here, to further investigate whether 20(S)-Rg3 could alter metabolism of SKOV3 cells *in vivo*, the subcutaneous tumors were fixated for confirmation by H&E staining and immunohistochemistry analysis of HK2 and PKM2. As shown in Fig. 5, subcutaneous tumors in control mice exhibited a significantly high level of HK2 and PKM2. Contrarily, tumors in 20(S)-Rg3-treated mice displayed a decrease of HK2 and PKM2. These *in vivo* findings coincided with the *in vitro* changes observed in the cell models, demonstrating that 20(S)-Rg3 robustly inhibited the Warburg effect in ovarian cancer.

Discussion

In this study, we demonstrated that 20(S)-Rg3, the pharmacologically active components of Panax ginseng, inhibited Warburg effect in ovarian cancer cells. The Warburg effect inhibited by 20(S)-Rg3 was accompanied by a decrease in levels of glucose uptake and lactate secretion as well as some metabolic enzymes in glycolysis including PKM2, HK2, GLUT1, and LDH. The expression of HK2 had the greatest reduction (Fig. 1). 20(S)-Rg3 downregulated p-STAT3 (Y705) without STAT3 in SKOV3 and 3AO cells, and overexpression of STAT3 can rescue the inhibitor effect induced by 20(S)-Rg3 (Figs. 3 and 4). We also found that 20(S)-Rg3 weakened HK2 and PKM2 *in vivo* through immunohistochemical staining of HK2, PKM2 in subcutaneous tumor samples (Fig. 5). Collectively, our data revealed that STAT3,

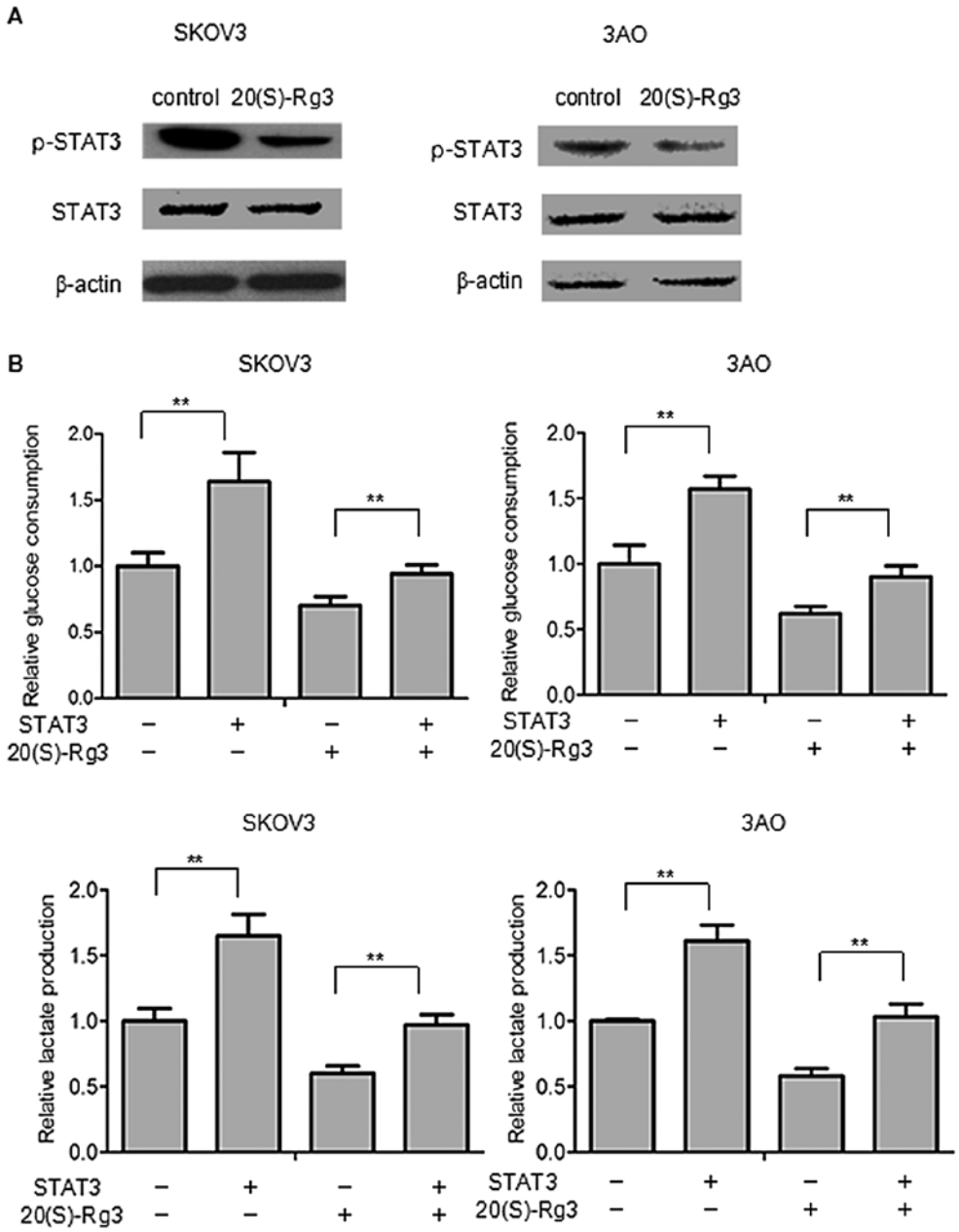

Figure 3. Downregulation of p-STAT3 contributes to the inhibition of Warburg effects by 20(S)-Rg3 in SKOV3 and 3AO cells. (A) Western blot assays show that the expression of p-STAT3 but not the signal transducer and activator of transcription 3 (STAT3) is upregulated in SKOV3 and 3AO cells treated by 20(S)-Rg3 for 48 h. (B) SKOV3 and 3AO cells expressing negative control, overexpression of STAT3 and STAT3 plus 20(S)-Rg3 were cultured for 48 h. Levels of lactate in the culture medium and glucose consumption were then measured and normalized to the cell number. All of the treatments in this figure were carried out in triplicate, and the results are the means ± standard deviation (SD). $^{**}P<0.01$, t-test.

has important roles in mediating 20(S)-Rg3-induced inhibition of aerobic glycolysis in ovarian cancer cells.

The Warburg effect not only allows cancer cells to meet their high energy demands and supply the anabolic precursors for nucleotide and lipid synthesis. The importance of Warburg effect in survival and proliferation of cancer cells in the tumour microenvironment is well documented. In this study, we have demonstrated for the first time that the ginsenoside 20(S)-Rg3, isolated from the traditional Chinese herb Panax ginseng, effectively inhibits aerobic glycolysis by inducing p-STAT3 inactivation in ovarian cancer cells.

Substantial research has been performed on the antitumor effect of 20(S)-Rg3, but the specific mechanism is still unclear. 20(S)-Rg3 has a broad spectrum of antitumor activities, ranging from the prevention of tumor growth and the inhibition of tumor progression to the enhancement of chemotherapeutic response. 20(S)-Rg3 has been shown to restrain HT29 colorectal cancer cell proliferation by inhibiting mitosis and inducing apoptosis (8). Kim *et al* demonstrated that 20(S)-Rg3 sensitized prostate cancer cells to docetaxel and other chemotherapeutics by inhibiting cell growth and augmenting apoptosis via suppression of constitutively activated and TNFα-induced NF-κB (26). 20(S)-Rg3 promoted TRAIL-induced apoptosis in hepatocellular carcinoma cells via C/EBP homology protein-mediated DR5 upregulation (27). Collectively, these findings, together with our *in vitro*

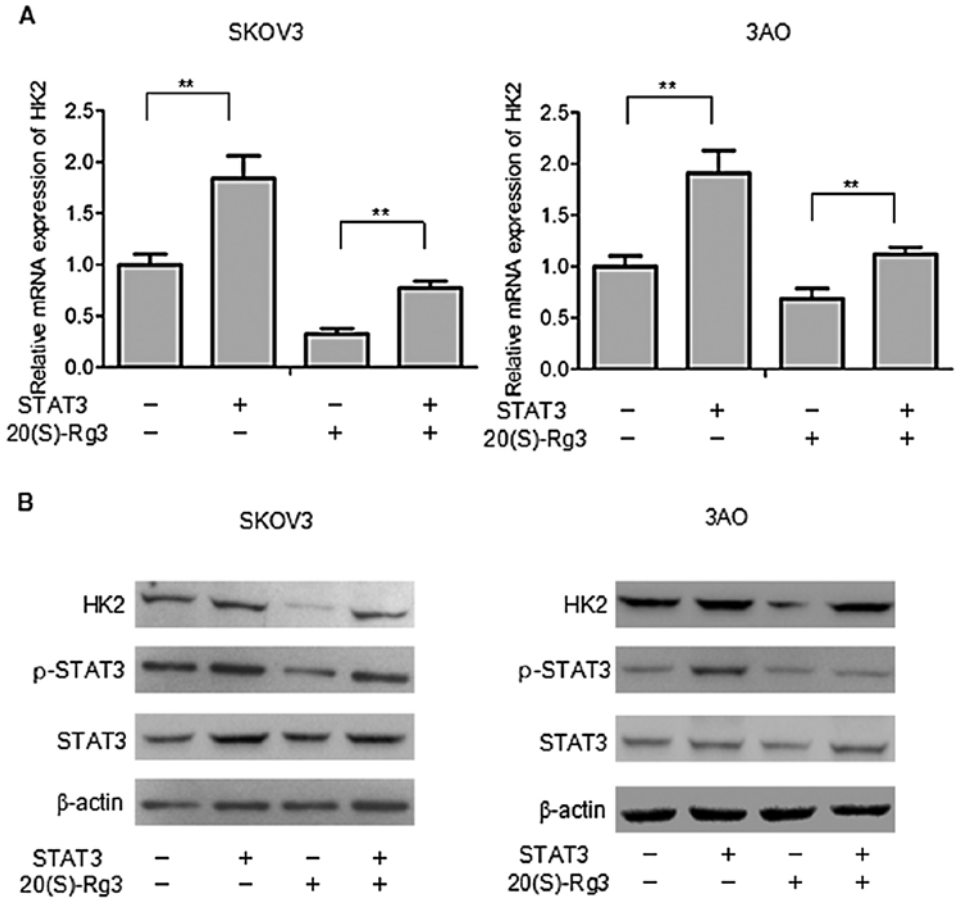

Figure 4. Downregulation of p-STAT3 contributes to the inhibition of Warburg effects by 20(S)-Rg3 in SKOV3 and 3AO cells. (A) Real-time RT-PCR analysis shows that the expression of hexokinase 2 (HK2) in SKOV3 and 3AO cells treated by negative control, overexpression of signal transducer and activator of transcription 3 (STAT3) and STAT3 plus 20(S)-Rg3 for 24 h. (B) Western blot assays show the expression of HK2 in SKOV3 and 3AO cells treated by negative control, overexpression of STAT3 and STAT3 plus 20(S)-Rg3 for 48 h. All of the treatments shown in this figure were carried out in triplicate, and the results are the means ± standard deviation (SD). $^{**}P<0.01$, t-test.

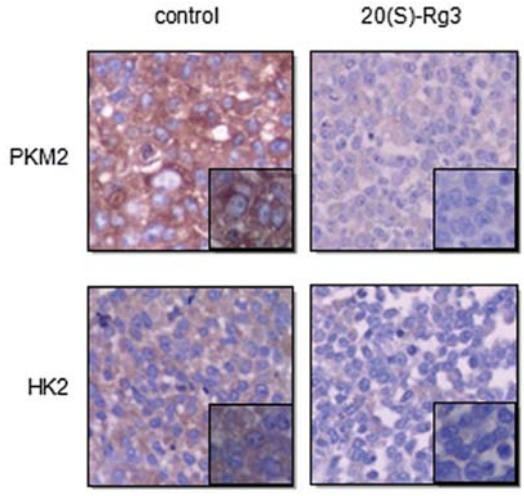

Figure 5. Expression of hexokinase 2 (HK2) and pyruvate kinase M2 (PKM2) in ovarian cancer tissue subcutaneous tumors of nude mice. Immunohistochemical staining of HK2, PKM2 and expression in subcutaneous tumor samples (original magnification, x200; insets, x400). 20(S)-Rg3 weakened HK2 and PKM2 *in vivo*. Values are presented as the means ± SD. $P<0.05$, $P<0.01$, for t-test.

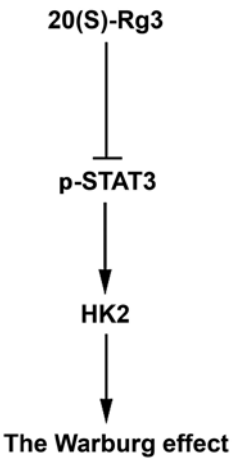

Figure 6. Schematic representation of the mechanism for 20(S)-Rg3-regulated metabolic switch.

and *in vivo* data, shed new light on the metabolic mechanism of ginsenosides in general, and validate potential clinical use of 20(S)-Rg3 in particular as an adjuvant chemotherapeutic for patients with advanced ovarian cancer.

STAT3 is associated with cell proliferation, survival, and carcinogenesis. Numerous studies have reported that STAT3 is constitutively phosphorylated in a wide variety of cancers through the increased activities of positive regulators, such

as the IL-6 cytokines, receptor tyrosine kinases EGFR and VEGFR (28). It has been reported that IL-6-STAT3 signaling pathway can affect glycolysis through regulating HK2 and PFKFB3 (25). It has also been reported that in breast cancer cells, the activation of STAT3 can combine to HK2 promoter, and then promote HK2 transcription activation, regulate aerobic glycolysis of breast cancer cells (21). HK2 is overexpressed in tumors and contributes to aerobic glycolysis. Thus, it is characterized as a pivotal player in the Warburg effect and an emerging target for cancer metabolism therapeutics (29,30). Our results showed that Warburg effect was inhibited by 20(S)-Rg3 though STAT3/HK2 pathways (Fig. 6). The experimental results confirmed our hypothesis, providing the first experimental demonstration that Warburg effect is inhibited by 20(S)-Rg3 through downregulating p-STAT3. Futhermore, we also found that 20(S)-Rg3 decreased metabolic enzymes in glycolysis including PKM2, HK2, GLUT1, and LDH, but the mechanism still needed further study. Our data lay the foundation for necessary additional studies of this compound to warrant its clinical use as a new anti-cancer drug for the treatment of various diseases including ovarian cancer.

Acknowledgements

We thank Ms. Yan Zhang, Ms. Jing Li, and Dr Mei Xue for technical assistance. This study was supported by the National Natural Science Foundation of China (Beijing, China) (no. 30973429).

References

1. Cho KR and Shih IeM: Ovarian cancer. Annu Rev Pathol 4: 287-313, 2009.
2. Swisher EM, Taniguchi T and Karlan BY: Molecular scores to predict ovarian cancer outcomes: a worthy goal, but not ready for prime time. J Natl Cancer Inst 104: 642-645, 2012.
3. Siegel R, Naishadham D and Jemal A: Cancer statistics, 2013. CA Cancer J Clin 63: 11-30, 2013.
4. Gillis CN: Panax ginseng pharmacology: a nitric oxide link? Biochem Pharmacol 54: 1-8, 1997.
5. Liao B, Newmark H and Zhou R: Neuroprotective effects of ginseng total saponin and ginsenosides Rb1 and Rg1 on spinal cord neurons in vitro. Exp Neurol 173: 224-234, 2002.
6. Nag SA, Qin JJ, Wang W, Wang MH, Wang H and Zhang R: Ginsenosides as anticancer agents: in vitro and in vivo activities, structure-activity relationships, and molecular mechanisms of action. Front Pharmacol 3: 25, 2012.
7. Lü JM, Yao Q and Chen C: Ginseng compounds: an update on their molecular mechanisms and medical applications. Curr Vasc Pharmacol 7: 293-302, 2009.
8. Lee SY, Kim GT, Roh SH, *et al*: Proteomic analysis of the anti-cancer effect of 20S-ginsenoside Rg3 in human colon cancer cell lines. Biosci Biotechnol Biochem 73: 811-816, 2009.
9. Mochizuki M, Yoo YC, Matsuzawa K, *et al*: Inhibitory effect of tumor metastasis in mice by saponins, ginsenoside-Rb2, 20(R)- and 20(S)-ginsenoside-Rg3, of red ginseng. Biol Pharm Bull 18: 1197-1202, 1995.
10. Bae EA, Kim EJ, Park JS, Kim HS, Ryu JH and Kim DH: Ginsenosides Rg3 and Rh2 inhibit the activation of AP-1 and protein kinase A pathway in lipopolysaccharide/interferon-gamma-stimulated BV-2 microglial cells. Planta Med 72: 627-633, 2006.
11. Keum YS, Han SS, Chun KS, *et al*: Inhibitory effects of the ginsenoside Rg3 on phorbol ester-induced cyclooxygenase-2 expression, NF-kappaB activation and tumor promotion. Mutat Res 523-524: 75-85, 2003.
12. Cui W, Cheng L, Hu C, Li H, Zhang Y and Chang J: Electrospun poly(L-lactide) fiber with ginsenoside rg3 for inhibiting scar hyperplasia of skin. PLoS One 8: e68771, 2013.
13. Yue PY, Wong DY, Wu PK, *et al*: The angiosuppressive effects of 20(R)-ginsenoside Rg3. Biochem Pharmacol 72: 437-445, 2006.
14. Warburg O: On the origin of cancer cells. Science 123: 309-314, 1956.
15. Kim JW and Dang CV: Cancer's molecular sweet tooth and the Warburg effect. Cancer Res 66: 8927-8930, 2006.
16. Vander Heiden MG, Cantley LC and Thompson CB: Understanding the Warburg effect: the metabolic requirements of cell proliferation. Science 324: 1029-1033, 2009.
17. Diaz N, Minton S, Cox C, *et al*: Activation of stat3 in primary tumors from high-risk breast cancer patients is associated with elevated levels of activated SRC and survivin expression. Clin Cancer Res 12: 20-28, 2006.
18. Germain D and Frank DA: Targeting the cytoplasmic and nuclear functions of signal transducers and activators of transcription 3 for cancer therapy. Clin Cancer Res 13: 5665-5669, 2007.
19. Wang SW and Sun YM: The IL-6/JAK/STAT3 pathway: Potential therapeutic strategies in treating colorectal cancer (Review). Int J Oncol 44: 1032-1040, 2014.
20. Zhu Q, Hu J, Meng H, Shen Y, Zhou J and Zhu Z: S-phase cell cycle arrest, apoptosis, and molecular mechanisms of aplasia ras homolog member I-induced human ovarian cancer SKOV3 cell lines. Int J Gynecol Cancer 24: 629-634, 2014.
21. Jiang S, Zhang LF, Zhang HW, *et al*: A novel miR-155/miR-143 cascade controls glycolysis by regulating hexokinase 2 in breast cancer cells. EMBO J 31: 1985-1998, 2012.
22. Demaria M, Giorgi C, Lebiedzinska M, *et al*: A STAT3-mediated metabolic switch is involved in tumour transformation and STAT3 addiction. Aging (Albany NY) 2: 823-842, 2010.
23. Sawayama H, Ishimoto T, Sugihara H, *et al*: Clinical impact of the Warburg effect in gastrointestinal cancer (Review). Int J Oncol 45: 1345-1354, 2014.
24. Kiuchi N, Nakajima K, Ichiba M, *et al*: STAT3 is required for the gp130-mediated full activation of the c-myc gene. J Exp Med 189: 63-73, 1999.
25. Ando M, Uehara I, Kogure K, *et al*: Interleukin 6 enhances glycolysis through expression of the glycolytic enzymes hexokinase 2 and 6-phosphofructo-2-kinase/fructose-2,6-bisphosphatase-3. J Nippon Med Sch 77: 97-105, 2010.
26. Kim SM, Lee SY, Cho JS, *et al*: Combination of ginsenoside Rg3 with docetaxel enhances the susceptibility of prostate cancer cells via inhibition of NF-kappaB. Eur J Pharmacol 631: 1-9, 2010.
27. Lee JY, Jung KH, Morgan MJ, *et al*: Sensitization of TRAIL-induced cell death by 20(S)-ginsenoside Rg3 via CHOP-mediated DR5 upregulation in human hepatocellular carcinoma cells. Mol Cancer Ther 12: 274-285, 2013.
28. Liu CY, Tseng LM, Su JC, *et al*: Novel sorafenib analogues induce apoptosis through SHP-1 dependent STAT3 inactivation in human breast cancer cells. Breast Cancer Res 15: R63, 2013.
29. Mathupala SP, Ko YH and Pedersen PL: Hexokinase-2 bound to mitochondria: cancer's stygian link to the 'Warburg Effect' and a pivotal target for effective therapy. Semin Cancer Biol 19: 17-24, 2009.
30. Vander Heiden MG, Lunt SY, Dayton TL, *et al*: Metabolic pathway alterations that support cell proliferation. Cold Spring Harb Symp Quant Biol 76: 325-334, 2011.